Journal of Microelectronics and Electronic Packaging (2024) **21**, 9–13

ISSN: 1551-4897

Stereolithographic Process for Embedding of Electronic Components into Multimaterial Flexible and Stretchable Polymer Substrate to Reduce Stress During Stretching

Tobias Tiedje*, Christoph Bräuer, Marco Luniak, Krzysztof Nieweglowski, and Karlheinz Bock

***Abstract*—The integration of rigid electronic components into stretchable materials is a complex challenge due to contrary material properties. This paper shows a novel approach for the embedding of electronic components into flexible and stretchable polymer substrates using a stereolithographic process that leads to stress reduction during stretching. The key factor is multimaterial printing with various elastic material properties. The paper shows a miniaturized packaged component (e.g., 0201 LED) in a flexible and stretchable substrate based on three different materials. The first material has rigid properties (stiffness 42.25 N/mm) and surrounds a small area of the LED with about 500 μm peripheral frame. The main purpose of this material is to round up the sharp edges of the LED to the next material. The second material is more elastic (stiffness 0.11 N/mm) and surrounds the first embedded LED. The purpose of the implementation of the second intermediate material is to spread the load between the LED and stretchable substrate caused by stretching. The third material has even higher elastic properties (stiffness 0.05 N/mm) and builds up the main part of the stretchable substrate (size of (4.5 × 34 × 0.27) mm^3). After the fabrication of the multimaterial substrate with the embedded LED, horseshoe conductive traces are screen printed with conductive paste. Finally, the embedded LED substrate with the conductive traces is cured at 125°C. The final stretchable substrate with the embedded LED is able to stretch up to about 25% for 30 cycles without disturbing the electrical function.**

***Keywords*—Components, embedded, multimaterials, stress relief, flexible, substrates, stretchable, SLA printing, wearables**

Introduction

Within the last decade, more and more wearables such as smartwatches or biomedical devices like new ear aids have been developed and brought to market. In the case of the smartwatch, there is a rigid electronic part and a flexible and stretchable arm strap to make it wearable. To achieve a possible higher level of wearing comfort, it would be desirable to integrate the rigid electrical components directly into the flexible and stretchable substrate.

The manuscript was received on November 15, 2023; revision received on February 15, 2024; accepted on February 15, 2024.

The original version of this paper was presented at the 56th International Symposium on Microelectronics (IMAPS'2023), San Diego, CA, USA, October 3-5, 2023.

TU Dresden - Institute of Electronic Packaging Technology, Technische Universität Dresden, Helmholtzstr. 10, Dresden 01062, Germany

*Corresponding author; email: tobias.tiedje@tu-dresden.de

The challenge arises from the fundamental differences in mechanical properties between rigid electronic components such as microcontrollers, typically made from traditional semiconductor materials, ceramic resistors or capacitors, rigid substrates, and the need for flexible and stretchable formable shapes for wearable electronics. Integrating rigid components into stretchable substrates demands innovative approaches that preserve the integrity and functionality of both elements.

In the field of research, different approaches have been performed. In the work, Schubert et al. [1] stretchable printed Ag- and Pt-conductive traces on a flexible and stretchable substrate with assembled LEDs have been explored. Hirman et al. [2] analyze the difference between nonconductive adhesives and electrically conductive adhesives for the connection of SMD chip components on flexible substrates.

This work shows an approach that uses multiple materials to embed the rigid components into a stretchable substrate with different stiffness properties to reduce the stress around the rigid electrical components and the connection to the conductive traces during the stretching. It also allows higher miniaturization of the devices, especially in their height, because the components are embedded in the substrate and the highest part defines the resulting thickness.

Concept

Fig. 1 shows the principle manufacturing method of the multimaterial approach using a stereolithographic printer (SLA). Firstly, the component is placed upside down on a temporary bonding foil, which is UV-transparent for the curing process. The contact pads are not sticking to the foil. Secondly, a liquid SLA-printable material with rigid properties is deposited like a glop top on the component. The printer uses a digital light processing unit, so only specific areas are cured. The printer cures the resin close to the component and the resin cross-links in rigid areas. The exposure time defines the thickness of the cured area. By choosing the right exposure time, the layer thickness can be matched with the height of the component. In the fourth step, the noncured residual liquid is removed. In the next steps, the semiflex and the flex material are applied analogously to steps two to four. However, the heights are manufactured slightly higher in comparison with the rigid area height. In the last step, the rigid material is applied, which levels the sample to the semiflex and flex materials. The sample is flipped and the rigid passivation layer is cured except for the pad areas

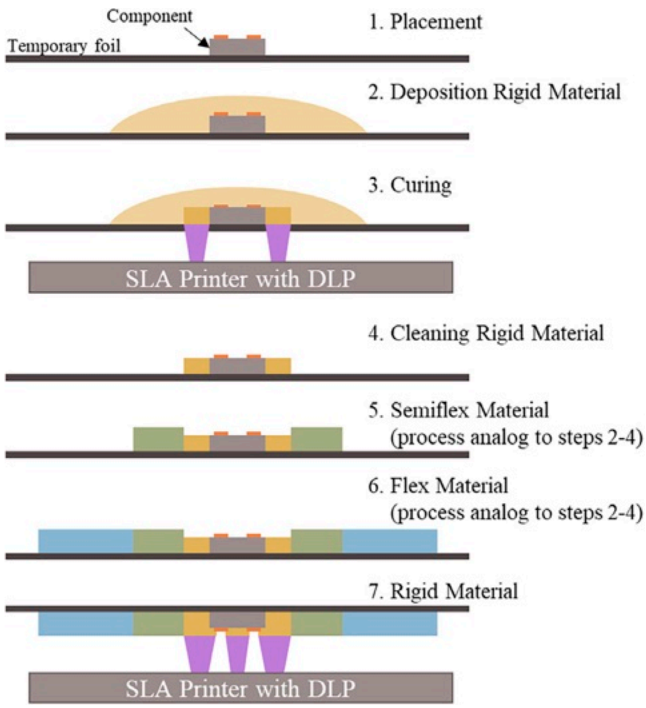

Fig. 1. Manufacturing of a multimaterial base substrate with embedded electronic components.

to keep blind holes for the conductive traces. In this process sequence, a multimaterial base substrate with embedded components can be achieved (also see Fig. 2a). The aim of the multimaterial approach is to reduce the stress between the rigid and flex materials to achieve high elongation during the stretching. The purpose of the rigid material is to round up the sharp edges of the electronic component. The semiflex material spreads the load between the rigid and the flex materials and the flex material has high elastic properties. Using this sequential printing build-up process, even more materials can be used to gradually change the transition between rigid and most stretchable materials. Furthermore, conductive traces can be added (see Fig. 2b) using screen printing, ink/aerosol-jetting, thin film processes, or another layer of the multimaterial with cavities that can be filled with conductive paste using a doctor blade approach. Finally, the temporary foil is removed.

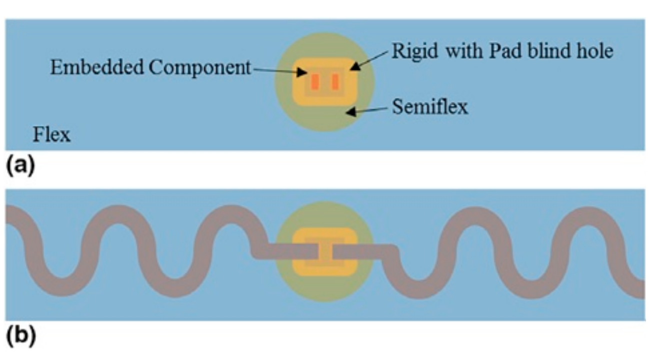

Fig. 2. Top view of: (a) base substrate with embedded component and (b) with conducted traces.

Table I
Used Materials and Mechanical Datasheet Properties

Name	Company – material name	Elongation at break (%)	References
Rigid	Formlabs – High Temp	3.3	[3]
Semiflex	BASF – Ultracur3D® FL 60	70	[4]
Flex	Formlabs – Elastic 50A	160	[5]
Silver paste	Dycotec – DM-SIP-2006	Stretchability up to 170	[6]

Methodology and Results

A. Materials and Modified SLA-Printer

Table I shows the used materials and their mechanical properties. The elongation at break gives an impression of the elastic properties of the different materials. The higher the elongation at break, the higher the elastic behavior of the material.

Fig. 3 shows a schematic of a modified SLA printer without the movable stage and build platform, which are common parts of a 3-D printer because they are not necessary for the manufacturing process. On top of the glass, the temporary foil with component and printable liquid is placed for curing (step 3 of Fig. 1). The camera system allows an alignment of the projected UV exposure pattern with the component on the temporary foil. The optical power at the surface of the glass is 1.9 mW/cm^2 (measurement: optical power meter PM400 with sensor S120VC from Thorlabs GmbH) [7].

B. Material Characterization

The elongations at break (datasheet values) in Table I show the elastic behavior of the materials. Due to different testing methods and sample thicknesses, these parameters can differ for specific applications. For this reason, stiffness analyses of the materials were done. Fig. 4 shows a test specimen with a thickness of 200 µm of the flex material manufactured with the modified SLA printer. The shape is according to type 5 of the norm for the determination of tensile properties for films and sheets (ISO 527-3 [8]).

Fig. 5a shows the used tensile test equipment with a linear unit to pull the specimen, a load cell to measure the force, and clamps to hold the specimen. Fig. 5b shows a stretched specimen of the flex material.

For every material, eight specimens have been manufactured and tested. Before testing, a preforce of about 1 N was applied to the specimen to ensure a straight specimen between the two

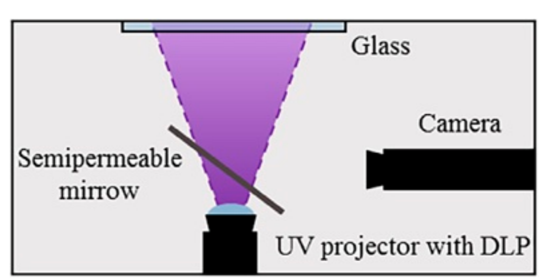

Fig. 3. Modified SLA printer with digital light processing and camera system and without movable stage and build platform.

Fig. 4. Test specimen according to DIN EN ISO 527-3 [8] with the shape of type 5 and thickness of 200 μm.

clamping positions. Fig. 6 (a) – (c) show the force-displacement diagrams of the materials flex, semiflex, and rigid.

The slope represents the stiffness k, which can be calculated with eq. (1),

$$k = \frac{F_{\max} - F_{\text{pre}}}{\Delta L} \quad (1)$$

with break force $F_{\max}$, preforce F_{pre}, and displacement length ΔL. It can be seen that the curves show a linear behavior and the slopes do not scatter too far apart (see also Table II stiffness). In Fig. 6c, the red curve shows plateau behavior. This occurs because the specimen has a higher break force than the measurement range of the load cell. Due to the manufacturing process, the specimens have inhomogeneities causing a higher scattering of the break force and the displacement length (see also Table II).

Table II summarizes the average values and the calculated stiffness with eq. (1) and the standard deviations of the materials.

The average displacement of the materials can be compared with the elongation at break of Table I, because the sample sizes of the test specimens are kept the same. Nevertheless, the datasheet values differ from the experimental results. This is caused by different testing methods used for the company datasheet values and different processing parameters, especially the curing conditions and the sample thicknesses. For the examined materials, the same processing parameters are chosen except for the exposure time of the materials to get the same sample thickness.

Fig. 7 shows the stiffness values of the different materials for equal sample thicknesses. These values show that rigid has a high stiffness and is about 400 times bigger than semiflex and semiflex is about twice as stiff as flex. To achieve a better

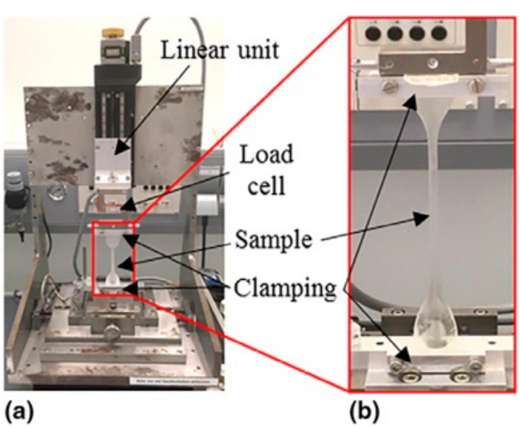

Fig. 5. (a) Tensile test equipment with flex specimen (no stretch) and (b) magnification flex specimen (stretched).

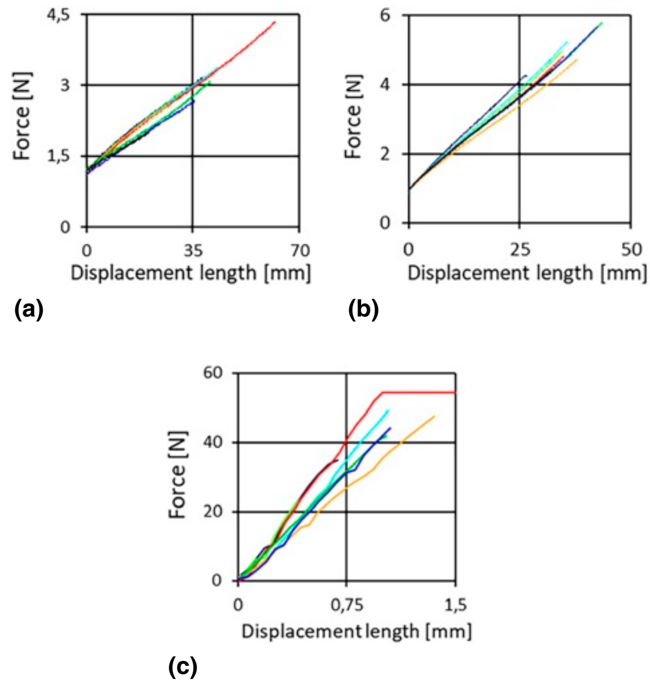

Fig. 6. Force-displacement diagrams: (a) flex, (b) semiflex, and (c) rigid.

transition between rigid and semiflex further materials can be added to the multimaterial base substrate.

C. Sample Manufacturing

Fig. 8 shows the manufacturing steps for a multimaterial substrate with an embedded 0201 LED and silver paste screen printing for the conductive traces. Fig. 8a shows the LED upside down, placed on the temporary bond foil. Fig. 8b shows the embedding of the LED after the rigid material is cured and cleaned. This represents steps two to four of Fig. 1. Fig. 8c shows the result after the processing of the semiflex material. In Fig. 8d, the processed flex material is shown (size of (4.5 × 34 × 0.27) mm^3). Fig. 8e shows the process step after printing the blind holes for the conductive traces of the rigid material. The conductive traces are printed with an MPM SPM screen printer and stainless-steel mesh Spoerl SD 45/18 on top of the base multimaterial substrate (shown in Fig. 8f). The screen printing is performed with a squeegee force of 45 N and squeegee speed of 15-18 mm/s. The silver paste is cured for 30 min at 125°C. Fig. 8g magnifies the connection area of the LED with the conductive traces.

D. Reliability Testing

Fig. 9a shows the test equipment for multimaterial substrates with embedded components. On one side, a rigid clamp bar is

Table II
Measured Mechanical Properties

Name	Average break force ± SD (N)	Average displacement ± SD (mm)	Average stiffness ± SD (N/mm)
Rigid	42.2 ± 9.4	1.0 ± 0.3	42.3 ± 5.7
Semiflex	4.9 ± 0.5	36.3 ± 5.0	0.1 ± 0.007
Flex	3.0 ± 0.6	37.7 ± 11.5	0.05 ± 0.005

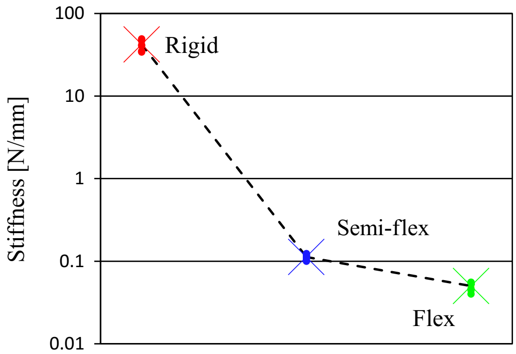

Fig. 7. Single and average stiffness (x) values of the examined materials.

visible and on the other side, a movable clamp bar is mounted on linear guidances. A linear unit is attached to the movable clamp, so it can drive the movable clamp back and forth. The samples are put in sample clamps with electrical connections (see Fig. 9c), which have a spring contact pin to ensure the electrical connection. On one clamp bar, up to six sample clamps can be mounted (see Fig. 9b with four samples mounted).

Fig. 10 shows a sample mounted in the reliability test setup before and after the stretching. The sample was able to stretch up to 25% without losing its electrical function.

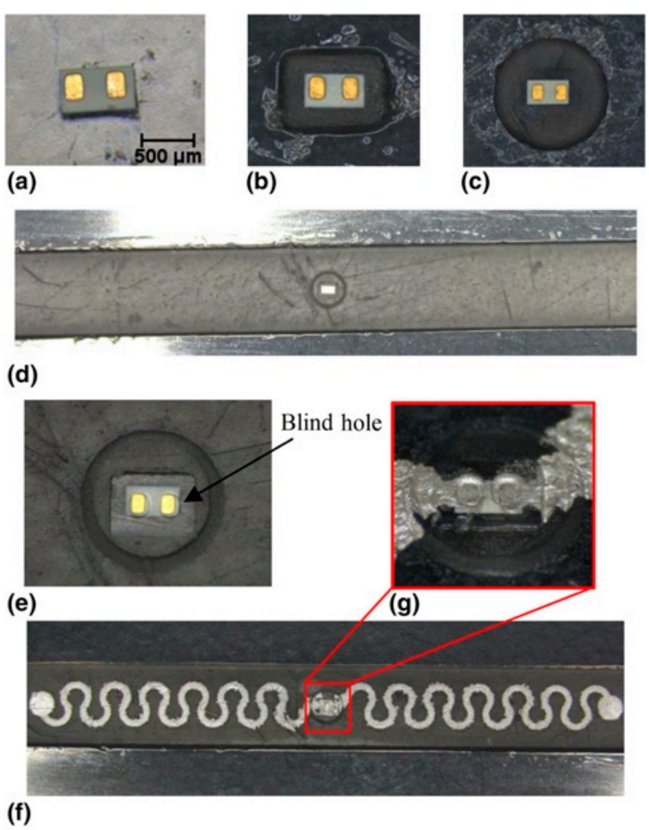

Fig. 8. Manufacturing steps of multimaterial substrate with an embedded 0201 LED: (a) LED placed on temporary foil, (b) cured rigid material, (c) cured semi-flexible material, (d) cured flexible material, (e) cured rigid layer for pad blind holes, (f) multimaterial substrate after silver screen printing, (g) magnification of LED pad connection.

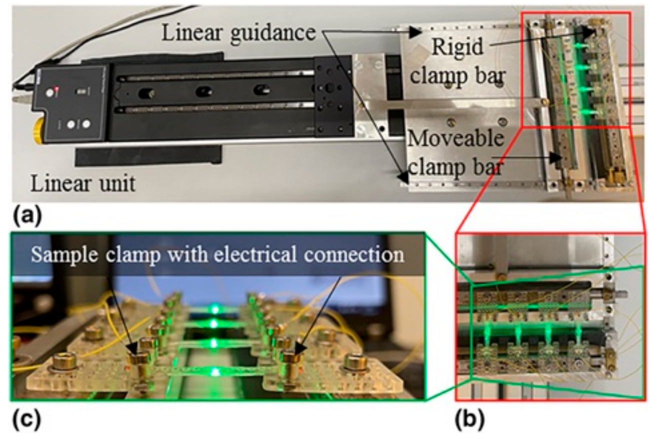

Fig. 9. Reliability test setup for multimaterial substrate with an embedded component: (a) Overview of reliability test setup for multimaterial substrate with an embedded component, (b) magnification and (c) side view of four mounted samples.

Fig. 11 shows the comparison of a single material substrate (flex) and a multimaterial substrate with each embedded LED during stretching. The single material substrate breaks directly on the LED edge. The multimaterial substrate withstands the strain due to the multimaterial approach, which reduces stress around the embedded component. The multimaterial substrates break in the flexible material according to the maximum breaking stress.

Table III shows the results of the reliability test with the electrical function of the LED. The cycles have been counted as long as the LED was continuously emitting. As soon as the LED begins to flicker, a degradation of the conductive trace is assumed. The results show 1,470 cycles for about 5.6% strain and 30 cycles for about 24.8% strain. The ultimate material strain is measured at 84.5% without electrical function and immediately before the multimaterial substrate cracks.

E. Glove Integration

Fig. 12 shows the manufacturing process for the integration of a 0201 LED into a nitrile glove using the multimaterial approach. Fig. 12a shows the result after the rigid and semiflex process. To measure e.g., a biomedical signal of a human, often the active side of a sensor component needs direct contact with the human body, as is done by a pulse oximeter. For this reason,

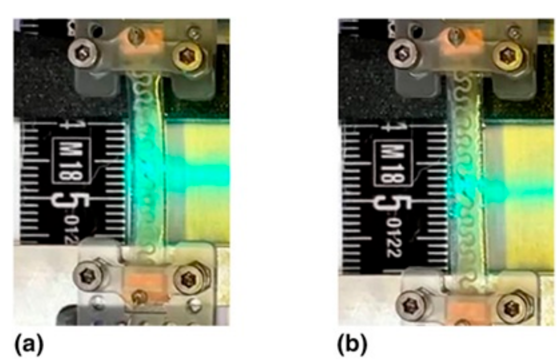

Fig. 10. Sample mounted in reliability test setup: (a) unstretched and (b) with about 25% strain.

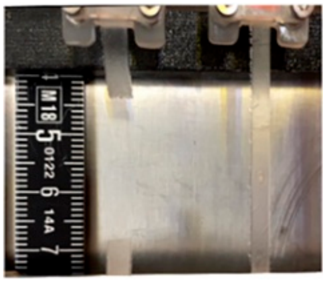

Fig. 11. Comparison of flex substrate (left) and multimaterial substrate (right) with embedded LED during stretching.

Table III
Reliability Results

Test condition	Strain (%)	Cycles
Multimaterial substrate with electrical function	5.8	1,470
	7.4	70
	15.2	40
	24.8	30
Multimaterial substrate without electrical function	84.5	-

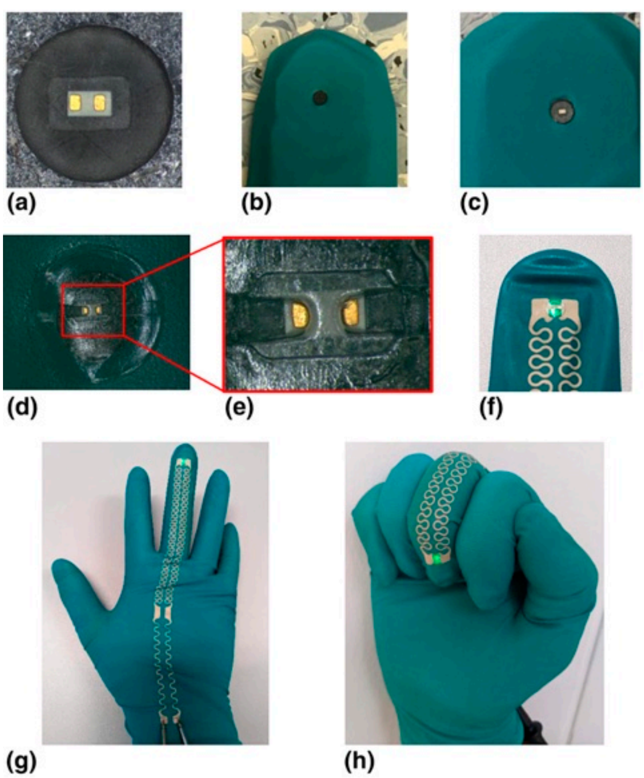

Fig. 12. Manufacturing steps of the integration of a 0201 LED into a nitrile glove using the multimaterial approach and functional test: (a) LED with cured rigid and semiflexible material, (b) punched hole in glove fingertip, (c) assembly of embedded LED into the glove, (d) cured flex material and additional cavity layer for silver paste with the three materials, (e) magnification of LED with rigid and semiflex cavity layer, (f) functional test after silver screen printing, dressed glove and functional test: straight (g) and bent position (h).

a hole is punched into one fingertip of the glove (shown in Fig. 12b) so that the active side of the LED faces inside the glove. Fig. 12c shows the assembly of the embedded LED into the glove. In Fig. 12d, the flex material is printed to connect the embedded LED to the glove and a cavity layer for the screen printing is processed with the three materials. The magnified view of cavities is shown in Fig. 12e. Finally, the screen printing and curing of silver paste are done and shown with a functional test in Fig. 12f. The Figs. 12g and 12h show the dressed glove in a function test in straight and bent positions. Six months after the manufacturing, the glove is still functional and can be bent. No degradation caused by the solvents of the silver paste on the used materials is observed.

Conclusion

This work shows a novel manufacturing method to embed electronic components in a stretchable substrate using a multimaterial approach and a stereolithographic process. It shows the detailed manufacturing process. The used substrate materials have been examined regarding their stiffness. The multimaterial approach is characterized by embedded 0201 LED components and their reliability tests show no functional degradation up to 25% strain for 30 cycles. Finally, a glove integration process of the LED for a possible biomedical application could be shown, enabling electrical functionality without any distortion.

Acknowledgments

The authors thank the financial support by the Federal Ministry of Education and Research of Germany in the program of “Souverän. Digital. Vernetzt.” Joint project 6G-life, project identification number: 16KISK001K.

References

[1] M. Schubert, L. Rebohle, Y. Wang, M. Fritsch, K. Bock, M. Vinnichenko, and T. Schumann, “Evaluation of nanoparticle inks on flexible and stretchable substrates for biocompatible application,” 2018 7th Electronic System-Integration Technology Conference (ESTC), pp. 1-6, Dresden, Germany, 18-21 September 2018.

[2] M. Hirman, J. Navrátil, F. Steiner, T. Džugan, and A. Hamácek, “Alternative technology for SMD components connection by non-conductive adhesive on a flexible substrate,” *Journal of Materials Science: Materials in Electronics*, Vol. 30, pp. 14214-14223, 2019.

[3] Formlabs, “MATERIAL DATA SHEET High Temp (2) [Datasheet],” [Online]. https://formlabs-media.formlabs.com/datasheets/High_Temp_Technical.pdf, 2018.

[4] BASF, “Technical Data Sheet Ultracur3D® FL 60 (3) [Datasheet],” [Online]. https://www.igo3d.com/mediafiles/Sonstiges/BASF/Ultracur3d/TDS/13.11.2020/Ultracur3D%20FL%2060_V3.0.pdf, 2020.

[5] Formlabs, “FLEXIBLE & ELASTIC RESIN Elastic 50A (1) [Datasheet],” [Online]. https://formlabs-media.formlabs.com/datasheets/2001420-TDS-ENUS-0.pdf, 2020.

[6] Dycotec, “DM-SIP-2006 (1) [Datasheet],” [Online]. https://www.dycotecmaterials.com/wp-content/uploads/2022/11/Dycotec-DM-SIP-2006-Datasheet-v1.0.pdf, 2022.

[7] T. Tiedje, K. Nieweglowski, and K. Bock, “Effects of silanated glass particles as photo resin filler to embed electronic components,” 2023 46th International Spring Seminar on Electronics Technology (ISSE), pp. 1-4, Timisoara, Romania, 10-14 May, 2023.

[8] ISO 527-3, *Plastics—Determination of Tensile Properties*, International Organization for Standardization, Burggrafenstraße 6 10787 Berlin, 2018.